Exploration of Airfoils: Lift, Drag and Stalling Characteristics at Altering Angles of Attack via Wind Tunnel Testing.

Keyvan Taghizadehasl, Izwan Bahar, Andy Jin

Abstract

In this experiment, the lift force, drag force and criterion for aerodynamic stalling of airfoils NACA 4412, NACA 23012, and NACA 63-210 are explored. These airfoils are tested in a wind tunnel at varying angles of attack and wind speeds in order to gain a better understanding of the influence of these two variable factors on the performance of airfoils and aerodynamic stalling. Additionally, the influence of vortex generators are infused into the scope of the experiment in an effort to gain a better understanding of factors that mitigate aerodynamic stalling.

Nomenclature

D	Drag
L	Lift
C_D	Coefficient of Drag
C_L	Coefficient of Lift
AOA	Angle of Attack
A	Wing Area
d	Density of Air
v	Velocity of Air

1. INTRODUCTION

The motivation behind the testing of the characteristics of Airfoils is derived from recent headlines relating to the industrial use of airfoils and the risks associated with their improper use. The recent crashes caused by the new Boeing 737 Max aircraft are a byproduct of pointing and aircraft at an improper angle of attack. The goal of this experiment is to explore the influence of air relative velocity, vortex generators and the angle of attack on aerodynamic stalling, lift and drag force generated.

In order to gain an understanding of the relationships that will be studied, 3 different airfoils will be tested: NACA 4412, NACA 63-210 and NACA 23012. These airfoils provide a diverse set of designs that allow the research team to have a larger domain to tests the influence of the impact of relative air velocity and angles of attack.

The objectives of this experiment are as follows:

(1) Depict the relationship between the angle of attack to the Lift and Drag Force generated.

(2) Portray the influence of the relative air velocity to the angle at which aerodynamic stalling occurs.

(3) Understand the impact of Vortex Generators on airfoils with respect to Lift, Drag and Aerodynamic Stalling.

2. Theory

Airfoil analysis provides a challenge since there are numerous factors in the performance of an airfoil. In this experiment, the factors relating to the design of the actual airfoil are not used as the variables; instead, the airfoils tested have the same surface area and outside variables, such as angle of attack and relative air velocity, are changed for analysis. In general, an airfoil functions by causing the air above its surface to travel at a faster rate than the bottom surface. Due to this, there is a pressure differential on the airfoil - higher pressure on the bottom and a lower pressure on the upper surface - via the venturi effect - causing an upward force called the lift force.

Loading… (1)

In addition to the lift force, there is a drag force associated with the airfoil. Drag force works in the opposite to the direction of the relative air velocity [1]. The equation of the drag force for airfoils is the following:

Loading… (2)

Both the equation for drag and lift force are dependent on the relative air velocity, the density of the atmospheric fluid wing area and their respective lift/drag coefficient, which are based on the shape of the airfoils. It is important to note that the Coefficient of Lift has a positive relationship with the angle of attack (generally for lower angles, then the relationship gets more complicated) [2]; additionally, with an increased angle of attack more of the profile of the airfoil is in the path of air causing higher drag on the foil. Therefore, one of the predictions of this experiment is that with the increase of the angle of attack and relative air velocity, the *magnitude* of the drag and lift force will increase.

Although the relationship insist on a positive relationship between angle of attack and force, there is a limit to this understanding. At a certain angle of attack aerodynamic stalling will take place. During an aerodynamic stall the boundary layer of air will separate from the airfoil and cease to create the pressure differential that drives the lift production on the airfoil. At this point instead of laminar flow over the trailing edge of the airfoil, vortices form at the start of the separation point and propagate down the airfoil. The prediction before the start of this lab is that the magnitude of the relative air velocity will not affect the location of aerodynamic stalling on the

airfoil, rather that this process is determined by the angle of attack.

In order to compare the results recorded from the experiment, a theoretical model is developed to conduct airfoil analysis. Using the Vortex Panel Method, a method that descretizes the shape of the airfoil into separate panels, the Kuta Condition, which is based on the assumption that there is a stagnation point at the trailing edge of the airfoil, in addition to utilizing the Thwaities' Method, which is used to determine the characteristics of laminar boundary layers, the theoretical coefficient of lift, drag, drag force, lift force, coefficient of pressure and stagnation points are determined via MATLAB Scripts.

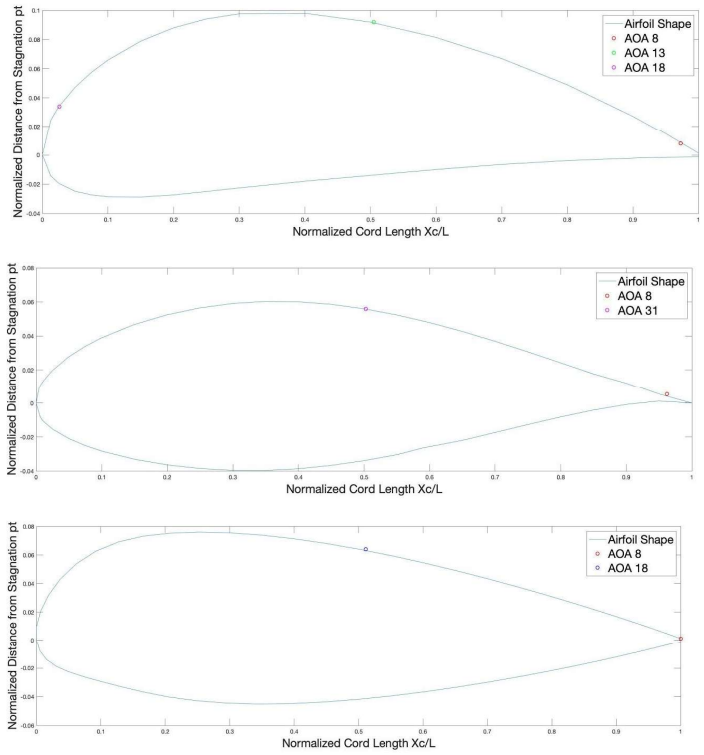

FIGURE 1: SHAPE OF NACA 4412, 63-210, 23012 RESPECTIVELY WITH THEORETICAL SEPARATION POINTS.

Figure 1 represents the shape of each airfoil and the theoretical angles of attack at which aerodynamic stalling will take place. According to the theoretical model, separation will take place at about an AOA of 18 degrees for NACA 4412, an AOA of 31 degrees for NACA 63-210 and an AOA of 18 degrees for NACA 23012. Therefore, it is predicted that the values of lift force generated will decrease starting at these angles of attack for each respective airfoil.

Vortex generators are also explored in this experiment. Vortex generators are relatively small fins placed near the leading edge of the airfoil in order to improve the overall aerodynamics of the system by delaying the point of separation. Therefore, it is predicted that the introduction of vortex generators will lead to aerodynamic stalling occur at higher angles of attack.

3. MATERIALS AND METHODS

During the experiment, materials and equipment used included the wind tunnel apparatus in room 70 of Hesse Hall (including parts like Emerson Varidyne 2 motor controller), lab computer, Berkeley-made strain gauge, weight hanger, calibration weights, Kanomax anemometer, smoke generator "Wizard Stick" toy by Zero Toys, custom-made wooden cut-out platforms for each airfoil, Johnson digital angle gauge, nuts, washers, bolts, NACA 4412, NACA 23012, NACA 63-210, and NACA 63-210 with vortex generators.

FIGURE 2: WIND TUNNEL APPARATUS IN ROOM 70 OF HESSE HALL

FIGURE 3: CLOSE-UP OF EMERSON MOTOR RPM CONTROLLER OF WIND TUNNEL

FIGURE 4: LAB VI ON COMPUTER SCREEN ACROSS FROM WIND TUNNEL

The custom lab started with calibration so that later data could be interpreted correctly.

Strain gauge detects force as electrical resistance, so it was used to sense the airfoil's reactions against the force applied by the wind. To use the strain gauge at max sensitivity, it had to be aligned parallel to the direction of the applied force (opposite being zero detection when perpendicular). Gravity, a downward force, was used to calibrate this. The strain gauge's angle (measured between the angle finder on the wind tunnel and a mark on the removable platform attached to the strain gauge device) was rotated to find when it peaked in output. The angle turned out to be about 2 degrees counterclockwise on angle finder. Given that the wind tunnel is designed and placed well - the wind's blowing direction inside should be perpendicular to gravity. So, strain gauge was then rotated 90 degrees clockwise (to translate to the wind direction, which is perpendicular to gravity), which is 88 degrees on the angle finder.

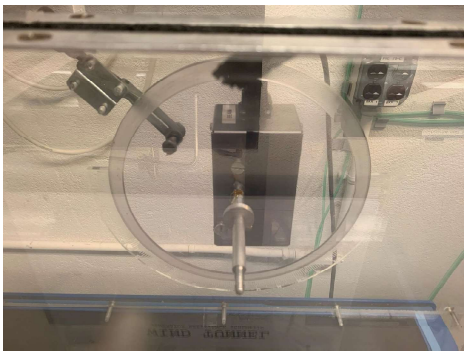

FIGURE 5: STRAIN GAUGE, ATTACHED TO CIRCULAR PLATFORM AND POLE, SECURED ONTO TEST SECTION, WITH ANGLE FINDER ON CIRCULAR PERIMETER

Kanomax anemometer was used to detect the wind speed based on fan motor RPM. The anemometer detects the heat transfer or loss from its hotwire when fluids such as the wind passes by. It was not suitable to put the Kanomax anemometer in the tunnel during the airfoil experiment because it would affect the wind movement across airfoil. Therefore, the correlation of the wind speed to fan RPM happened in controlled environment without airfoils. There are sliders with slim openings both vertically and horizontally on top of the wind tunnel test section. A special holder was used that could both hold the anemometer vertical through the wind tunnel (like a straw) and fit on the sliders. The anemometer is moved around to detect its relatively most sensitive position. Then, data was gathered from motor RPMs of 300, 400, 499, 599, 701, 800, 899, 999. It seemed deal when the anemometer was roughly centered on the test section. A plot mapping out the correlation was formed. In future trials with airfoil, this could be used to tell the wind speed based on motor speed.

FIGURE 6: HOT-WIRE, SPECIAL HOLDER, TEST SECTION SLIDERS, AND ANEMOMETER

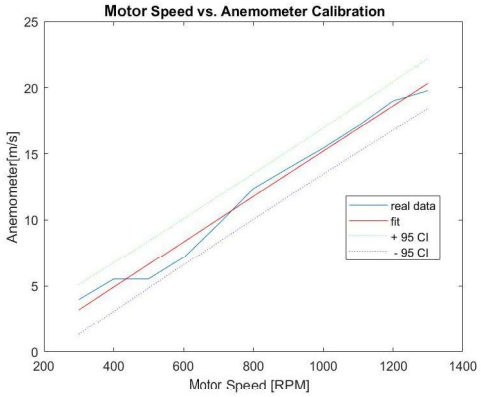

FIGURE 7: CORRELATION OF MOTOR RPM TO ANEMOMETER DETECTION OF WIND SPEED IN METERS PER SECOND

After positioning the strain gauge efficiently as calibrated earlier, its output was correlated with force using weights. First, a hanger was added on the pole of the strain gauge. Then, 5 grams of weight from 0 grams to 100 grams was added between each trial, and gathered 30 data points each time. The weight of the hanger parts was also measured and taken into account.

FIGURE 8: BOX OF CALIBRATION WEIGHTS WITH TWEEZERS

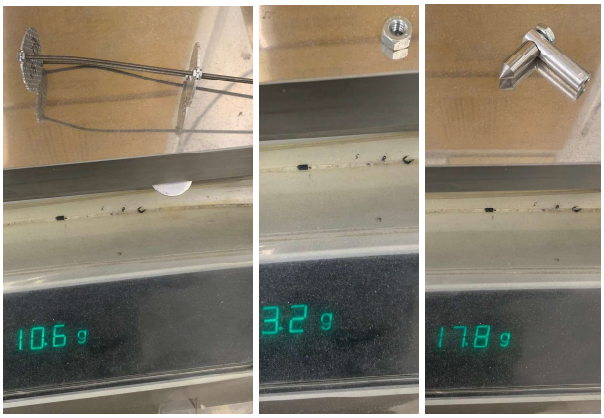

FIGURE 9: WEIGHING OF PARTS OF WEIGHT HANGER

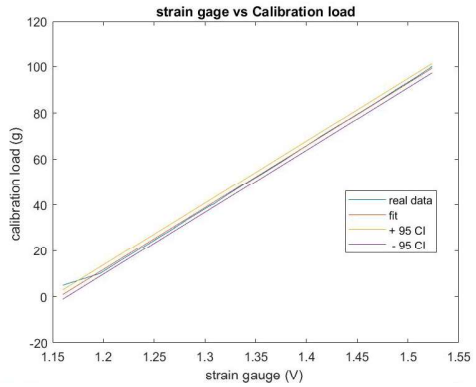

FIGURE 10: CORRELATION OF WEIGHT IN GRAMS TO STRAIN GAUGE OUTPUT IN VOLTS

Data gathering for airfoils started after the completion of calibration. The airfoils were designed to be 8 inches wide and about 7 inches long. The width is important because it should not be long enough on the strain gauge pole that it would interfere with the strain gauge wires. The length is important because it must fit through the circular entrance of the test section. The airfoils were printed with the same material and same printer, and a hole for the strain gauge pole was added at the airfoil's location of center of mass. After being printed, the airfoils are polished, especially at the edges where extra material lingered.

FIGURE 11: NACA 4412 3D PRINTED AIRFOIL BEFORE POLISH

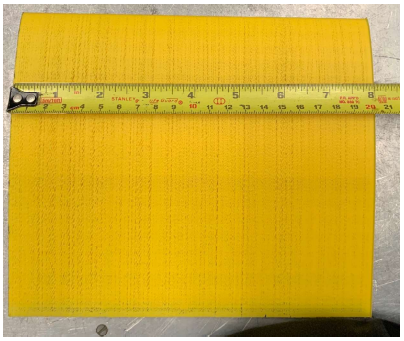

FIGURE 12: NACA 23012 3D PRINTED AIRFOIL BEING MEASURED

FIGURE 13: NACA 63-210 3D PRINTED AIRFOIL BEING TESTED

FIGURE 14: NACA 63-210 3D PRINTED AIRFOIL WITH VORTEX GENERATORS

Before the testing of each airfoil, a wooden cut-out platform is created in order to place the digital angle gauge parallel on top of the airfoil. The platform consists of two cut-outs bonded together with nuts and bolts, with rectangular pieces of foam taped on as cushions and place holders. The digital angle gauge is zeroed while placed upright on the surface of the test section. After securing the airfoil of interest onto the strain gauge pole using a washer and nut, the cut-out platform and then the digital angle gauge are placed on. The angle is adjusted The digital angle gauge actually contains a pendulum, so it uses gravity to detect the change in angle relative to its zeroed position. After shifting the airfoil to ± 0.1 degrees of the desired angle (one of 0, 5, 10, 12, 14, 15, 16, 18, 20, 23, 26, 30, or 36 degrees), the test section is closed and the motor is turned on. Using the Emerson Varidyne 2 motor controller of the wind tunnel apparatus, the motor RPM is adjusted to 499, followed by a brief pause to wait for the actual speed to catch up after turning on. At least 10 data points are taken, using a computer across from the wind tunnel, with caution in mind that the wind tunnel outputs data at a certain pace, so some collection while clicking too fast might not yield actual new data. Then, this process is repeated each time after increasing motor RPM to 599, 701, 800, 899, and 999. Then, this larger cycle is repeated after changing the angle. Between angle changes, confirmation is made that the airfoil did not move over 0.1 degrees. This is repeated in all the angles for both drag and lift, which are tested differently by rotating the strain gauge 90 degrees. Finally, this is all repeated for each of the three airfoils, plus the airfoil with vortex generators.

The impact of the weight of the airfoils are taken into account, by measuring the output of the strain gauge without wind due to purely the weight of the airfoils.

FIGURE 15: NACA 4412 IN TESTING WITH ITS CUT-OUT PLATFORM AND JOHNSON DIGITAL ANGLE GAUGE

Outside of statistical data analysis, visual experimentation using a smoke generator was done to confirm separation point and visualize airflow patterns and pressures. The smoke generator is a fairly cheap toy called “Wizard Stick” produced by Zero Toys. It is loaded up with non-toxic oil and plugged in to power. The toy is kept upright and when the trigger is held down, smoke is generated from the oil. A person holds the toy right next to the wind entrance of the wind tunnel, and aims it by looking into the wind tunnel through small gaps until the smoke visually splits over and under the airfoil.

FIGURE 16: “WIZARD STICK” SMOKE GENERATOR IN USE

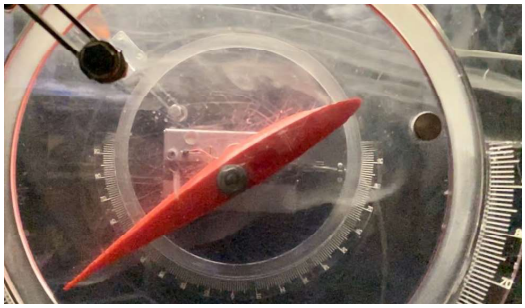

FIGURE 17: VORTICES REPRESENTED VISUALLY BY GENERATED SMOKE ABOVE NACA 63-210 AIRFOIL TILTED 30 DEGREES

The uncertainty has been included for all the plots. The uncertainties of the experiment can be detected during calibration plot of the strain gauge and wind speed, the deviation of data during repetition of experiment for each state, and also the uncertainty of the experiment outcome using Gauss' Method of Uncertainty Propagation. For the uncertainty in the calibrations, it is coming from taking linear fit from relationship of 2 sets of data. The linear fit assumption to get a calibration function produced certain uncertainty. These uncertainty can be gathered from using polyfit (3) and polyconf (4) function in matlab. The polyfit function will be used to get linear fit of data x and y relationship of degree n=1. Then, S output from polyfit can be used as input for polyconf for the error estimation. Polynomial p of degree n=1 collected from polyfit is used for polyconf to evaluate p at value X. The output of p and S is used by polyconf to generate 95% prediction intervals Y ± DELTA for new observations at the values in X. As a result, uncertainties DELTA is accumulated for the uncertainties in calibration plots. The same method is applied as well to see the data deviation from experiment repetition for each state.

[Loading… (3)
Loading… (4)

The uncertainty of the experiment outcome can be observed from using Gauss' Method of Uncertainty Propagation. In order to quantify the uncertainty in the measurement of the Lift Force (1) and Drag Force (2) based on measurements of wind speed uncertainty. From formula of lift force and drag force, partial derivative(5),(6) of wind speed is calculated and multiplied by the uncertainty of wind speed gathered from data propagation of wind speed measurement.

$$par\_V\_lift = d*v*A*C_L \quad (5)$$
$$par\_V\_drag = d*v*A*C_D \quad (6)$$

Then, from Gauss' Method of Uncertainty formula(7), the total uncertainty formula :

tot_unc_lift = Loading… (7)
tot_unc_drag = Loading… (8)

tot_unc_lift = total uncertainty of lift force
tot_unc_drag = total uncertainty of drag force
uncer_v = uncertainty of velocity from measurement
par_v_lift = partial derivative of velocity of lift force equation
par_v_drag=partial derivative of velocity of drag force equation

The result of the experiment for total uncertainty at 95% confidence interval will be in this format.

Lift_force = mean_lift_force ± tot_unc_lift @ 95% CI (9)
Drag_force = mean_drag_force ± tot_unc_drag @ 95% CI (10)

4. Results

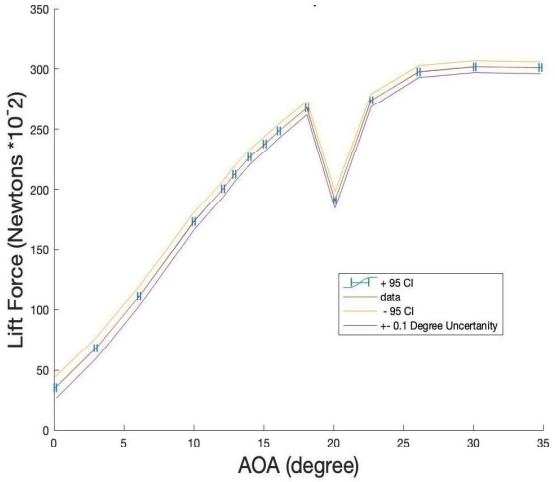

FIGURE 18: AOA vs LIFT FORCE - NACA 4412 AT 15.4 m/s.

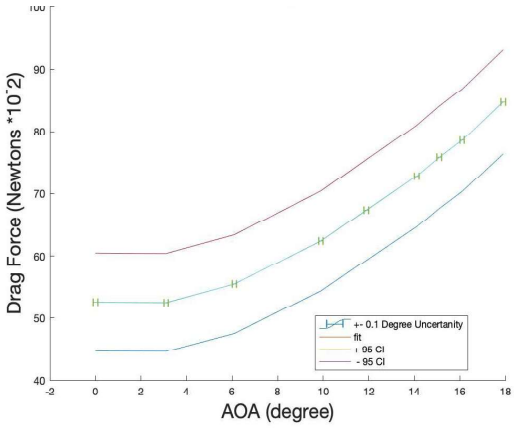

FIGURE 20: AOA vs DRAG FORCE - NACA 4412 AT 15.4 m/s.

**Note: With the exception of figures 18 and 20, all other figures mentioned in this section will be in the appendix.*

Figures 18 and 19 depict the point of aerodynamic stalling for NACA 4412 at different relative air velocities. Both figures depict a drop in lift force generation at 18.1 degrees angle of attack. Additionally, figures 20 and 21 depict the increase of the drag force with increased angle of attack and relative air velocity.

Figures 22 and 23 depict the point of aerodynamic stalling for NACA 63-210 at different relative air velocities. Both figures depict a drop in lift force generation at 24 degrees angle of attack. Additionally, figures 24 and 25 depict the increase of

the drag force with increased angle of attack and relative air velocity.

Figures 26 and 27 depict the point of aerodynamic stalling for NACA 63-210 with Vortex Generators at different relative air velocities. Both figures depict a drop in lift force generation at about 25 to 28 degrees angle of attack. Additionally, figures 28 and 29 depict the increase of the drag force with increased angle of attack and relative air velocity.

Figures 30 and 31 depict the point of aerodynamic stalling for NACA 23012 at different relative air velocities. Both figures hint at a drop in lift force generation at 15 degrees angle of attack but show a continuation in increased lift force generation with angle of attack. Additionally, figures 32 and 33 depict the increase of the drag force with increased angle of attack and relative air velocity.

5. DISCUSSION

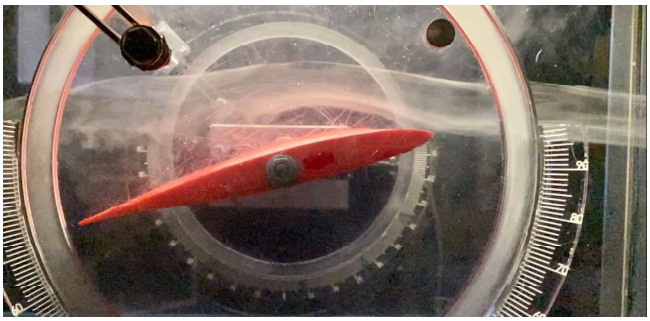

FIGURE 34: NACA 63-210 TESTING AT AOA 15 degrees.

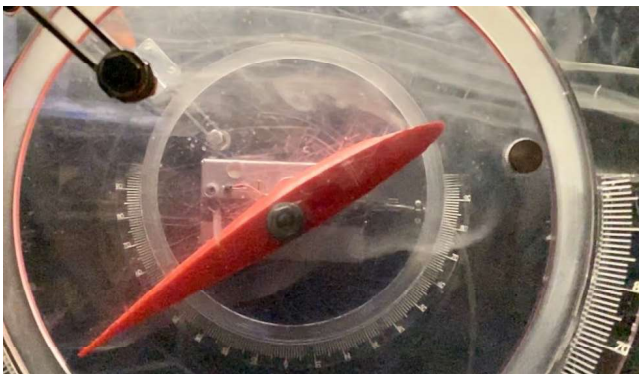

FIGURE 35: NACA 63-210 TESTING AT AOA 30 degrees.

Figures 34 and 35 are pictures of the airfoil NACA 63-210 testing at 15 and 30 degrees of AOA, respectively. From the results it can be seen that at 15 degrees the airfoil has yet not reached separation and the boundary layer (as depicted in Figure 34) sticks onto the airfoil though its length - generating lift at all points. However, in Figure 35, the separation has occurred since AOA is above 18, and vortices can be seen forming above the airfoil - ceasing the generation of lift.

It is important to note that the increase in lift force after the separation point shown in the AOA vs Lift Force plots provided in results is due to the nature of the design of testing, where after a certain angle the air from the wind tunnel will put the airfoil up and the strain gauge will incorrectly record it as upwards force; however this issue was noticed and addressed in interpreting the data and separation points.

Nearly all of the AOA vs Lift Force plots depict the predicted trend: the angle of attack that leads to separation (with some differences from the theoretical model) and that angle that these separation points occur at are independent of the relative air velocity - only the magnitude of the force is affected positively by the increase in air velocity.

Additionally, all of the AOA vs Drag Force plots follow the expected trend: with increased angle of attack and relative air velocity, the drag force is increased.

Comparing the AOA vs Lift Force results derived from NACA 63-210 (Figures 22, 23) and NACA 63-210 with vortex generators (figures 25, 26) depicts the impact of vortex generators on airfoils. With the addition of vortex generators the same airfoil, facing the same relative air velocity has its aerodynamic stall at a higher angle of attack. This trend stays consistent with the prediction that the addition of vortex generators will delay the angle at which stalling occurs, improving the aerodynamics of the airfoil and introducing a factor of safety for when in use.

The AOA vs Lift Force plots for NACA 23012 (Figures 30 and 31) show some ambiguity however. This is probably due to the poor quality of the 3D printed part that was tested for this airfoil design. Due to the very low infill (very light) and the porous skin the boundary layers did not behave as expected, yielding the results shown.

The results are within uncertainty bounds. The uncertainties of the experiment outcomes by using Gauss Method is plotted with the experiment result. The data does not deviate from the calculated uncertainty. It shows that the results are within expected uncertainty bounds.

There are many possible sources of error in calibration section. During the strain gauge angle calibration, the angle mark on wind tunnel has increments of 1 degree. Since the angle mark on wind tunnel 2significant figures, the accuracy of the reading is less accurate if to be compared with angle mark that has more than 2 significant figures. Therefore, it was roughly concluded to be 2 degrees with 2 significant figures to be the most efficient, with the best of our ability. During the anemometer calibration, hotwire was placed across the wind tunnel since wind speeds may vary at different parts of the test section, especially near the edges. The center of test section outputs the most efficient reading for the experiment. The rough centering of the anemometer might contribute some error. But, from the test that has been done across the wind tunnel section, the deviation of the wind speed is not too large. Fair assumption can be made that rough centering placement of anemometer does not contribute much on the error of wind speed reading. Then, airfoil production by using ultimaker 3D

printer does contribute to the resolution of the design produced. The low resolution of the 3D printer may affect the aerodynamics of the airfoil, seen in the porousness of the airfoil. This affects the flow of the wind hence affect the lift and drag force produced. The wind tunnel provided does not have the equipment to calculate moment of the airfoil. This shortcoming does not allowed more analysis to be done on the airfoil. The attachment between the airfoil and strain gauge apparatus is not very accurate and strong. After a few run of experiment, there was some error on the angle positioning of the airfoil. The angle either has been reduced or increased after running the experiment a few times. This does affect the angle of attack value that should be constant for that set of experiment, so we made sure between each angle change that the angle did not change over 0.1 degrees during data collection. Other than that, the theoretical model used for comparison is not accurate enough. It is because the theoretical model created is based on several assumptions such as Kuta condition and laminar flow for the Thwaities method that can introduce error into the experiment. The experiment data might be far from true value. But, during comparison between theoretical model and the experiment result, the expected outcome is very close to each other.

In order to mitigate these shortcomings in the future, a more accurate angle finder with more significant figures can be used during strain gauge calibration. The accuracy anemometer placement during wind speed calibration can be increased by having a custom made anemometer holder that is more strongly attached to the wind tunnel with high precision knob to adjust the position of the anemometer. This can produce more accuracy reading during calibration setup. Then, the attachment between airfoil and strain gauge can be improved by putting a lock features like a set screw or groove between the two item to reduce movement between them. The apparatus set up for this experiment is just depend on friction between the airfoil side and screw from the strain gauge tower. Last but not least, the assumption made for the theoretical model can be improved by figuring out more accurate model to follow in order to create a theoretical model that's close to the real value.

6. CONCLUSION

This experiment addressed the lift force, drag force and stalling of popular airfoils NACA 4412, NACA 23012, NACA 63-210, and NACA 63-210 variation with vortex generators using wind tunnel, with the idea in mind that all the characteristics mentioned plus vortex generators are especially important today in airplane industry and safety.

Results showed that aerodynamic stalling location depends on angle of attack - not relative air velocity, lift force increases as a function of air speed until stalling point, angle of attack and drag force have positive relation, and implementation of vortex generators increased the angle of attack to cause separation.

Possible improvements for this experiment include taking more data points per angle of attack, including more angles of attack, making the cut-out platforms more exacting, tightening the fit between hole in airfoil and strain gauge pole. Lots of these have to do with lab time constraints, especially for data taking since the ceiling is limited by the data output pace of the strain gauge, and our inexperience. Of course, there could also be improvement made through increasing the cost such as to improve the quality of the airfoils.

ACKNOWLEDGEMENTS

I would like to express my deepest appreciation to all those who provided us the possibility to complete this report. A special gratitude I give to our Professor Simo Makiharju whose contribution in stimulating suggestions and encouragement, helped me to coordinate our project especially in writing this report.

Furthermore I would also like to acknowledge with much appreciation the crucial role of the staff of Mr Daniel Paragas, Senior Lab Mechanician who gave the permission to use all required equipment and the necessary materials to complete the wind tunnel experiment. A special thanks goes to our GSIs who help us to organize and gave suggestions about this custom lab.

REFERENCES

[1] "Modern Lift Equation," *NASA*. [Online]. Available: https://wright.nasa.gov/airplane/lifteq.html.[Accessed: 08-Dec-2019].

[2]"Inclination Effects on Lift," *NASA*. [Online]. Available: https://www.grc.nasa.gov/WWW/K-12/airplane/incline.html. [Accessed: 08-Dec-2019].

[3]L. Zyga, "Vortex Generators," *Phys.org*, 13-Sep-2012. [Online].Available:https://phys.org/news/2012-09-scientists-purpose-vortex.html. [Accessed: 08-Dec-2019].

APPENDIX

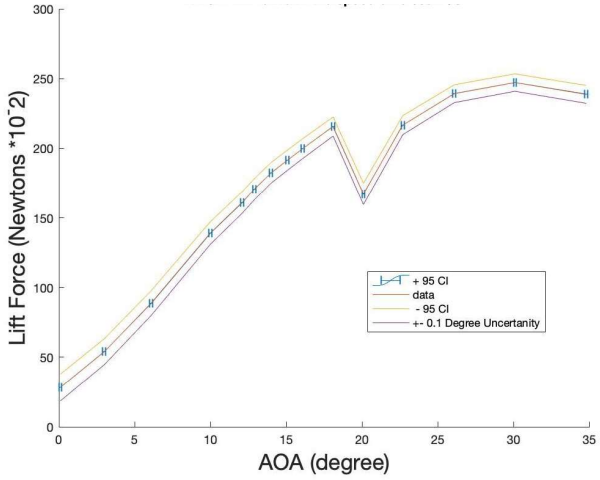

FIGURE 19: AOA vs LIFT FORCE - NACA 4412 AT 13.8 m/s.

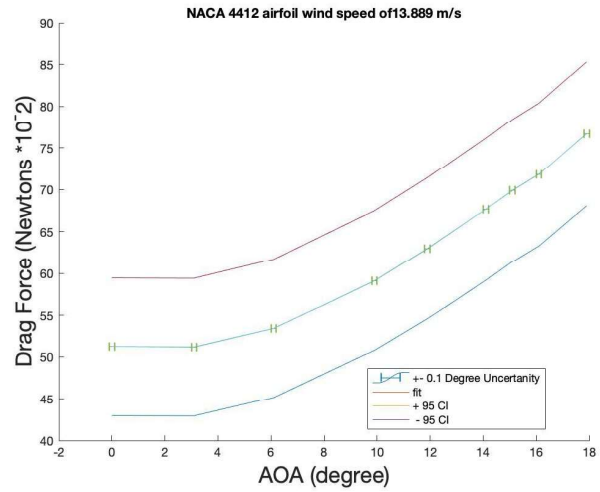

FIGURE 21: AOA vs Drag FORCE - NACA 4412 AT 13.8 m/s.

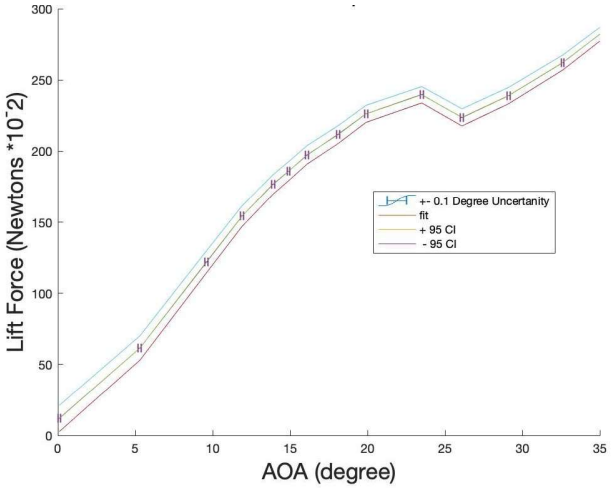

FIGURE 22: AOA vs LIFT FORCE - NACA 63-210 AT 15.4 m/s.

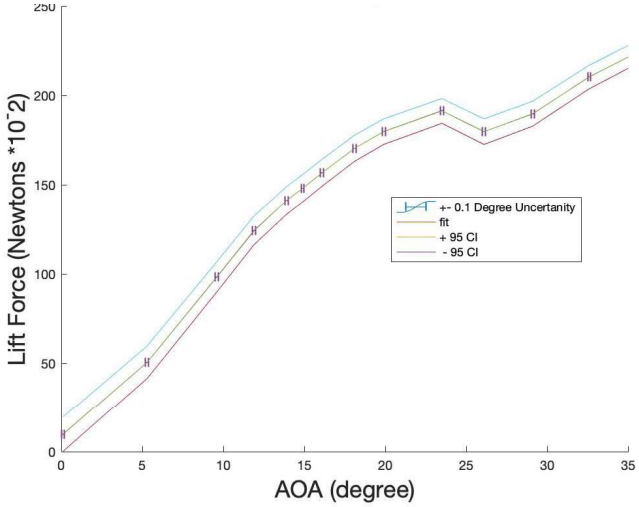

FIGURE 23: AOA vs LIFT FORCE - NACA 63-210 AT 13.8 m/s.

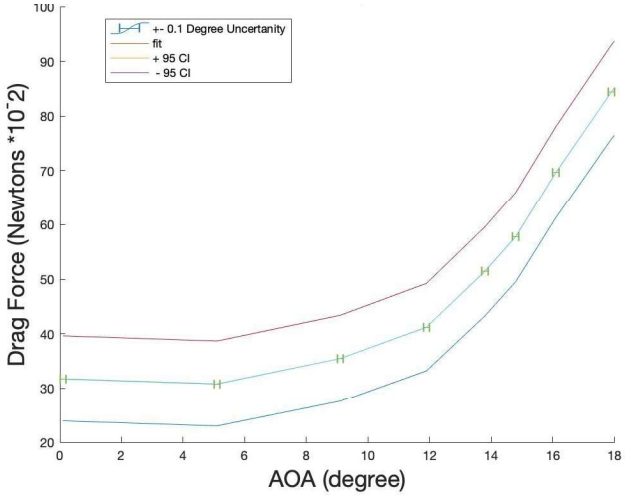

FIGURE 24: AOA vs DRAG FORCE - NACA 63-210 AT 15.4 m/s.

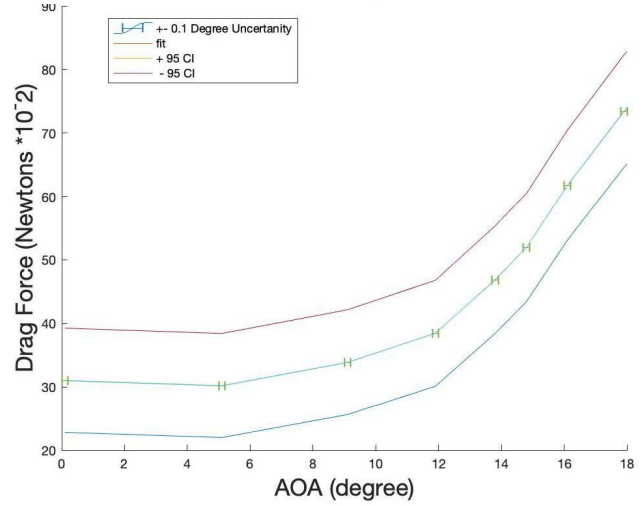

FIGURE 25: AOA vs DRAG FORCE - NACA 63-210 AT 13.8 m/s.

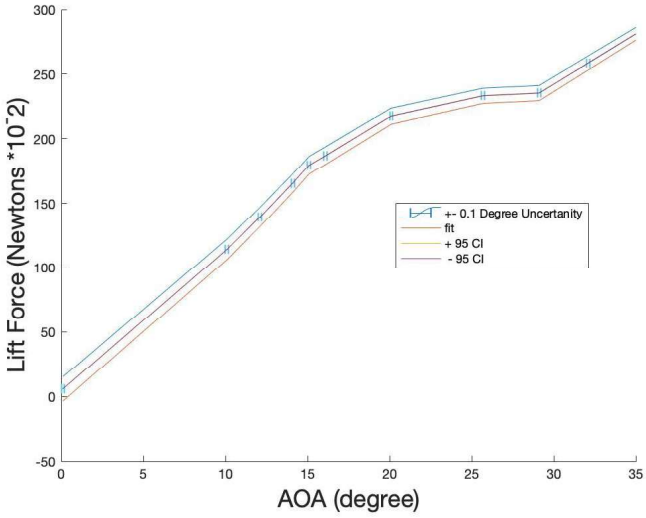

FIGURE 26: AOA vs LIFT FORCE - NACA 63-210 VORTEX GENERATOR AT 15.4 m/s.

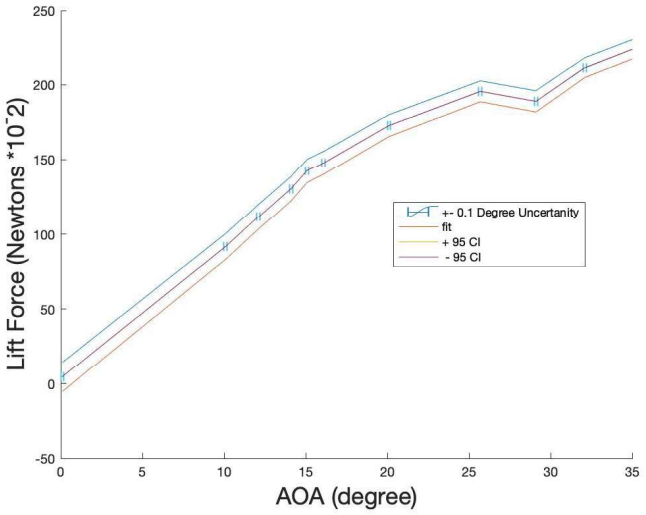

FIGURE 27: AOA vs LIFT FORCE - NACA 63-210 VORTEX GENERATOR AT 13.8 m/s.

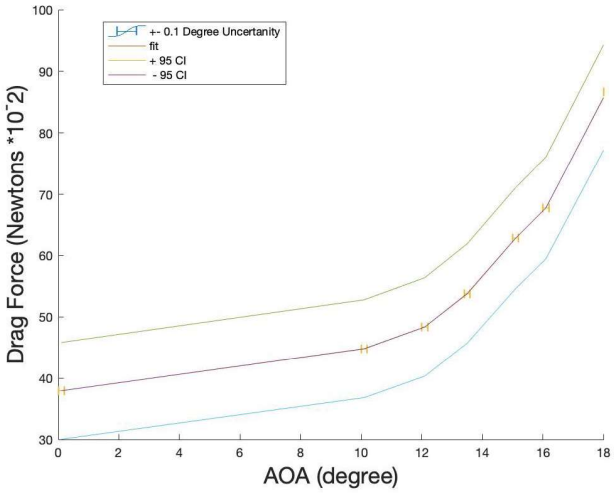

FIGURE 28: AOA vs DRAG FORCE - NACA 63-210 VORTEX GENERATOR AT 15.4 m/s.

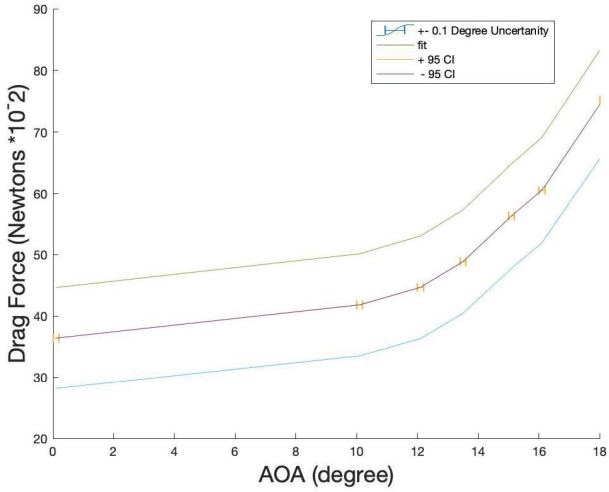

FIGURE 29: AOA vs DRAG FORCE - NACA 63-210 VORTEX GENERATOR AT 13.8 m/s.

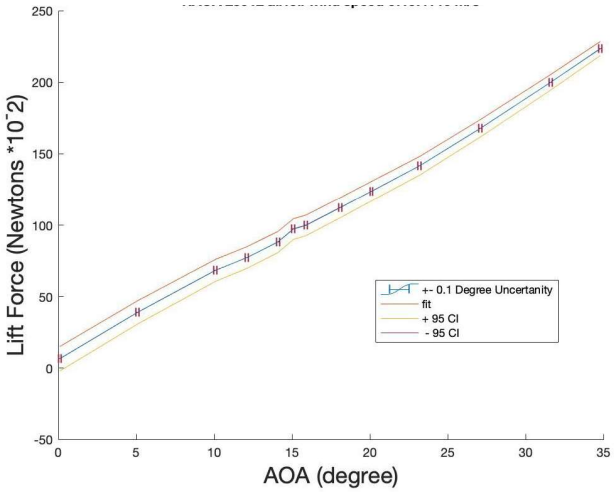

FIGURE 30: AOA vs LIFT FORCE - NACA 23-012 AT 15.4 m/s.

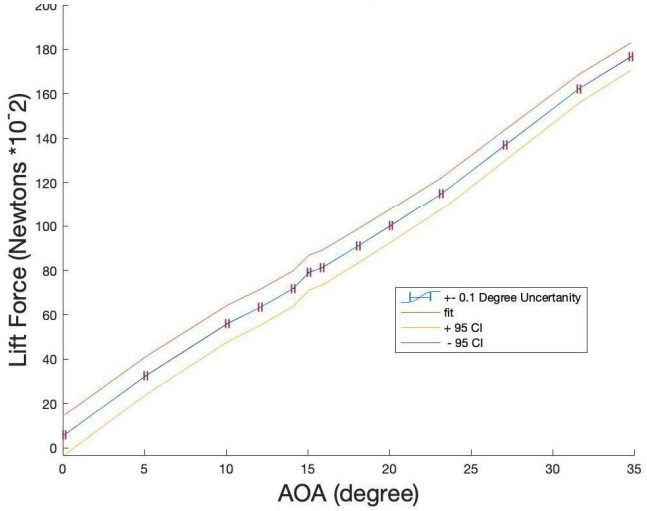

FIGURE 31: AOA vs LIFT FORCE - NACA 23012 AT 13.8 m/s.

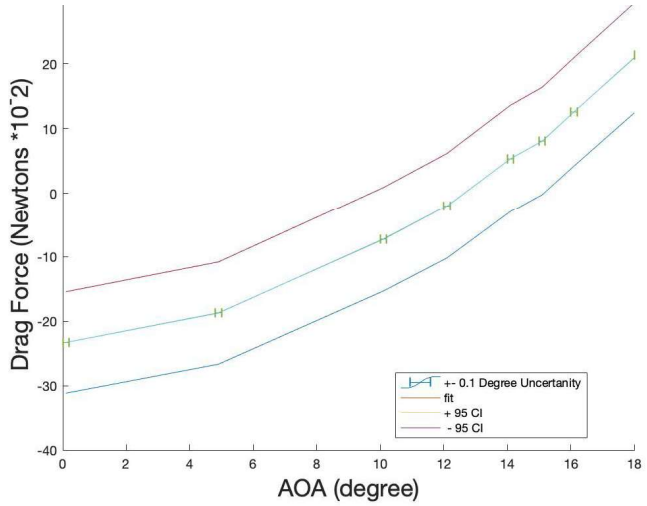

FIGURE 32: AOA vs DRAG FORCE **-** NACA23012 AT 15.4 m/s.

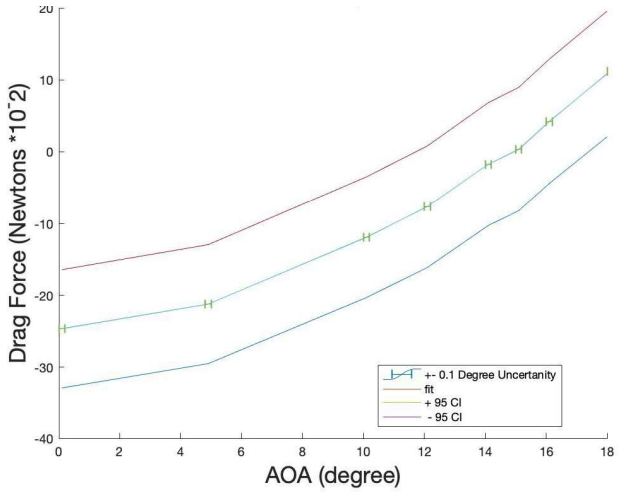

FIGURE 33: AOA vs DRAG FORCE **-** NACA 23012 AT 13.8 m/s.